Sentinel-6 Michael Freilich and Jason-3 Tandem Flight Exploitation (S6-JTEX)

Final Report

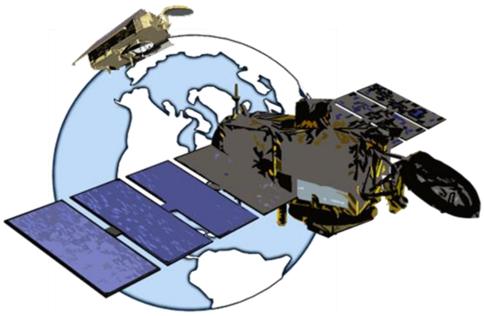

CLS-ENV-NT-24-0139

V1.0 – 22/04/2024

Open/Public/Público

11 rue Hermès, Parc Technologique du Canal — 31520 Ramonville Saint-Agne, France

Tel +33 (0)5 61 39 47 00 Fax +33(0)5 61 75 10 14

www.cls.fr

CHRONOLOGY ISSUES/HISTORIQUE DES VERSIONS

Issue/ Version	Date	Object/Objet	Written by/ Rédigé par	Checked by / Vérifié par	Approved by/ Approuvé par
1.0	22/04/2024	First version	T.Moreau (CLS) and S6-JTEX Team	T. Moreau (CLS)	C. Donlon (ESA)

DISTRIBUTION/LISTE DE DIFFUSION

Company/Organisme	Means of distribution/ Format de diffusion	Names/Destinataires
ESA	Notification	C. Donlon, A. Egido
CLS	Notification	L. Amarouche, E. Cadier, S. Labroue, A. Mangilli, T. Moreau, P. Prandi, N. Taburet, P. Thibaut, N. Tran
Aresys	Notification	P. Guccione, L. Recchia
NOC	Notification	C. Gommenginger, B. Timmermans
Magellium	Notification	M. Ablain
TUM	Notification	M. Passaro, F. Schlembach, J. Oelsmann, D. Dettmering
Univ. Porto	Notification	J. da Silva, A. Ferreira, J. Magalhaes

LIST OF CONTENTS/SOMMAIRE

LIST OF TABLES

LIST OF FIGURES

REFERENCE DOCUMENTS

Abdalla, S., S. Dinardo, “Does swell impact SWH from SAR altimetry?”, in SAR Altimetry Workshop, La Rochelle, France, Oct. 31, 2016.

Ablain, M., et al., Benefit of a second calibration phase to estimate the relative global and regional mean sea level drifts between Sentinel-6 Michael Frielich and Jason-3, to be submitted.

Altiparmaki, O., Kleinherenbrink, M., Naeije, M., Slobbe, C., & Visser, P. (2022). Sar altimetry data as a new source for swell monitoring. Geophys. Res. Lett.. doi: 10.1029/2021GL096224.

Amarouche, L., Thibaut, P., Zanife, O.Z., Dumont, J.P., Vincent, P., Steunou, N., 2004. Improving the Jason-1 ground retracking to better account for attitude effects. Mar. Geod. 27 (1–2), 171–197. https://doi.org/10.1080/01490410490465210.

Amarouche, L., Tran, N., Herrera, D., Guerin, C.-A., Dubois, P., Aublanc, J., Boy, F., 2019. Impact of the ocean waves motion on the Delay/Doppler altimeters measurements. OSTST Meeting 2019, Chicago, Illinois, United States, Oct. 21–25. in Ocean Surface Topography Science Team Meeting 2014. Available online at https://ostst.aviso.altimetry.fr/fileadmin/user_upload/OSTST2019/IPM_05_Amarouche_DopplerWavesSARMode_OSTST2019_Final.pdf

Amarouche, L., N. Tran, M. Mrad, T. Pirotte, H. Etienne, T. Moreau, F. Boy, C. Maraldi, C. Donlon, A. Egido, Analysis of the sea state impact on Sentinel-6MF Delay/Doppler measurements, to be submitted.

Amraoui, S.; Guccione, P.; Moreau, T.; Alves, M.; Altiparmaki, O.; Peureux, C.; Recchia, L.; Maraldi, C.; Boy, F.; Donlon, C. Optimal Configuration of Omega-Kappa FF-SAR Processing for Specular and Non-Specular Targets in Altimetric Data: The Sentinel-6 Michael Freilich Study Case. *Remote Sens.* 2024, *16*, 1112. https://doi.org/10.3390/rs16061112.

Aouf, L. and Phalippou, L., “On the signature of swell for the Cryosat-2 SAR-mode wave data”, in Ocean Surface Topography Science Team Meeting 2015. Available online at https://meetings.aviso.altimetry.fr/fileadmin/user_upload/tx_ausyclsseminar/files/OSTST2015/IPM-02-ostst_Aouf_sarmode_2015_1.pdf.

Benveniste J., Birol F., Calafat F., Cazenave A., Dieng H., Gouzenes Y., Legeais J.F., Léger F., Niño F., Passaro M., Schwatke C., Shaw A., 2020. (The Climate Change Initiative Coastal Sea Level Team): Coastal sea level anomalies and associated trends from Jason satellite altimetry over 2002–2018. Nature Scientific Data, 7, 357. https://doi.org/10.1038/s41597-020-00694-w.

Boisot, O., L. Amarouche, J-C. Lalaurie and C-A. Guérin, 2016, “Dynamical Properties of Sea Surface Microwave Backscatter at Low-Incidence: Correlation Time and Doppler Shift,” IEEE Trans. Geosci. Remote Sens., 54, 7385-7395, https://doi.org/10.1109/TGRS.2016.2601242.

Boy, F., Desjonquères, J.-D., Picot, N., Moreau, T., Raynal, M., 2017. CRYOSAT-2 SAR Mode Over Oceans: Processing Methods, Global Assessment and Benefits. IEEE Trans. Geosci. Remote Sens. 55, 148-158. https://doi.org/10.1109/TGRS.2016.2601958.

Buchhaupt, C., Fenoglio-Marc, L., Dinardo, S., Scharroo, R. and Becker, M., 2018. A fast convolution based waveform model for conventional and unfocused SAR altimetry. Advances in Space Research, 62(6), pp.1445-1463. https://doi.org/10.1016/j.asr.2017.11.039.

Buchhaupt, C. 2019. Model Improvement for SAR Altimetry. Ph.D. Thesis. Darmstadt, Schriftenreihe Fachrichtung Geodäsie der Technischen Universita¨t Darmstadt, ISBN 978-3-935631-44-0. https://tuprints.ulb.tu-darmstadt.de/9015/.

Cadier, E. et al., Leveraging Sentinel-6A interleaved mode to characterize High Resolution error budget over ocean. In Ocean Surface Topography Science Team Meeting 2022. Doi: 10.24400/527896/a03-2022.3423.

Cadier, E., Courcol, B., Prandi, P., Quet, V., Moreau, T., Maraldi, C., Bignalet-Cazalet, F., Dinardo, S., Martin-Puig, C., Donlon, C., Assessment of Sentinel-6MF low resolution numerical retracker over ocean: continuity on reference orbit and improvements, submitted in Adv. Space Res.

Cipollini P., Benveniste J., Birol F., Joana Fernandes M., Obligis E., Passaro M., Strub T., Valladeau G., Vignudelli S., Wilkin J., 2017. Satellite Altimetry in Coastal Regions. In: Stammer D. and Cazenave A. (Eds.), Satellite Altimetry Over Oceans and Land Surfaces. doi: 10.1201/9781315151779-11.

Clerc, S., Donlon, C., Borde, F., Lamquin, N., Hunt, S.E., Smith, D., McMillan, M., Mittaz, J., Woolliams, E., Hammond, M., Banks, C., Moreau, T., Picard, B., Raynal, M., Rieu, P., Guérou, A. Benefits and Lessons Learned from the Sentinel-3 Tandem Phase. Remote Sens. 2020, 12, 2668. https://doi.org/10.3390/rs12172668.

Dinardo, S., B. Lucas and J. Benveniste, SAR altimetry at 80 Hz, in Ocean Surface Topography Science Team Meeting 2014. Available online at https://meetings.aviso.altimetry.fr/fileadmin/user_upload/tx_ausyclsseminar/files/SAR_Altimetry_at_80_Hz_OSTST_2014.pdf.

Dinardo, S., Maraldi, C., Cadier, E., Rieu, P., Aublanc, J., Guerou, A., Boy, F., Moreau, T., Picot, N., and Scharroo, R., 2023. Sentinel-6 MF Poseidon-4 radar altimeter: Main scientific results from S6PP LRM and UF-SAR chains in the first year of the mission, Advances in Space Research, https://doi.org/10.1016/j.asr.2023.07.030.

Donlon C., Cullen R., Giulicchi L., Vuilleumier P., Francis R., Kuschnerus M., Simpson W., Bouridah A., Caleno M., Bertoni R., Rancaño J., Pourier E., Hyslop A., Mulcahy J., Knockaert R., Hunter C., Webb A., Fornari M., Vaze P., Brown S., Willis J., Desai S., Desjonqueres J.D., Scharroo R., Martin-Puig C., Leuliette E., Egido A., Smith W., Bonnefond P., Le Gac S., Picot N., Tavernier G., 2021, The Copernicus Sentinel-6 mission: Enhanced continuity of satellite sea level measurements from space, Rem. Sens. Env., 258. https://doi.org/10.1016/j.rse.2021.112395.

Egido, A., Smith, W.H.F., 2017. Fully focused SAR altimetry: theory and applications. IEEE Trans. on Geosci. Remote Sens. 55 (1), 392–406. https://doi.org/10.1109/TGRS.2016.2607122.

Egido, A.; Smith, W.H.F. Pulse-to-Pulse Correlation Effects in High PRF Low-Resolution Mode Altimeters. IEEE Transactions on Geoscience and Remote Sensing, 2019a, 57, 2610–2617. doi:10.1109/TGRS.2018.2875622.

Egido, A., Ray, C., “On the Effect of Surface Motion in SAR Altimeter Observations of the Open Ocean”, in Ocean Surface Topography Science Team Meeting 2019b. Available online at https://ostst.aviso.altimetry.fr/fileadmin/user_upload/OSTST2019/IPM_03_Egido20191022_-_OSTST_-_AEE.pdf.

Egido A., Buchaupt C., Feng H., Ray C., Smith W., Vendarmark D., Development of Fully-Focused SAR Altimetry for Oceanographic Applications, in Ocean Surface Topography Science Team Meeting 2020, Available online at: https://meetings.aviso.altimetry.fr/fileadmin/user_upload/tx_ausyclsseminar/files/20201018_-_OSTST_-_AEE_01.pdf

Egido, A., Dinardo, S., Ray, C., 2021. The case for increasing the posting rate in delay/doppler altimeters. Adv. Space Res. 68 (2), 930–936. https://doi.org/10.1016/j.asr.2020.03.014.

Egido A., Buchhaupt C., Boy F., Maraldi C. and CLS Team, Correcting for the Vertical Wave Motion Effect in S6-MF Observations of the Open Ocean, in Ocean Surface Topography Science Team Meeting 2022. DOI: 10.24400/527896/a03-2022.3460.

Gommenginger, C. Martin-Puig, L. Amarouche, and R. K. Raney, Review of State of Knowledge for SAR Altimetry over Ocean, Version 2.2, EUMETSAT, EUM/RSP/REP/14/74930421, November 2013.

Hernández-Burgos, S., et al., "A Fully Focused SAR Omega-K Closed-Form Algorithm for the Sentinel-6 Radar Altimeter: Methodology and Applications," in *IEEE Transactions on Geoscience and Remote Sensing*, vol. 62, pp. 1-16, 2024, Art no. 5206016, doi: 10.1109/TGRS.2024.3367544.

Kleinherenbrink, M., Naeije, M., Slobbe, C., Egido, A., Smith, W., 2020. The performance of CryoSat-2 fully-focussed SAR for inland water-level estimation, Remote Sensing of Environment, Volume 237, 111589, ISSN 0034-4257, https://doi.org/10.1016/j.rse.2019.111589.

J. M. Magalhaes and J. C. B. da Silva, "Satellite Altimetry Observations of Large-Scale Internal Solitary Waves," in *IEEE Geoscience and Remote Sensing Letters*, vol. 14, no. 4, pp. 534-538, April 2017, doi: 10.1109/LGRS.2017.2655621.

Magalhaes, J. M., Alpers, W., Santos-Ferreira, A. M., & Da Silva, J. C. (2021). Surface wave breaking caused by internal solitary waves effects on radar backscattering measured by SAR and radar altimeter. Oceanography, 34(2). https://doi.org/10.5670/oceanog.2021.203.

Magalhaes, J.M.; Lapa, I.G.; Santos-Ferreira, A.M.; da Silva, J.C.B.; Piras, F.; Moreau, T.; Amraoui, S.; Passaro, M.; Schwatke, C.; Hart-Davis, M.; et al. Using a Tandem Flight Configuration between Sentinel-6 and Jason-3 to Compare SAR and Conventional Altimeters in Sea Surface Signatures of Internal Solitary Waves. *Remote Sens.* 2023, *15*, 392. https://doi.org/10.3390/rs15020392.

A. Mangilli, P. Thibaut, C. R. Duguay and J. Murfitt, "A New Approach for the Estimation of Lake Ice Thickness From Conventional Radar Altimetry," in *IEEE Transactions on Geoscience and Remote Sensing*, vol. 60, pp. 1-15, 2022, Art no. 4305515, doi: 10.1109/TGRS.2022.3186253.

Mangilli, A., Duguay, C., Murfitt, J., Sree Mugunthan, J., Moreau, T., Amraoui, S., Thibaut, P., Donlon, C., Improving the Estimation of Lake Ice Thickness with High Resolution Radar Altimetry Data, submitted in Remote Sens.

Moreau, T., Tran, N., Aublanc, J., Tison, C., Le Gac, S. and Boy, F., 2018. Impact of long ocean waves on wave height retrieval from SAR altimetry data. Advances in Space Research, 62(6), pp.1434-1444. https://doi.org/10.1016/j.asr.2018.06.004.

Moreau, T., and S6JTEX Team, Sentinel-6 Michael Freilich and Jason-3 Tandem Flight Exploitation (S6-JTEX) study, in Ocean Surface Topography Science Team Meeting 2023. DOI: 10.24400/527896/a03-2023.3829.

Nilsson, J., Forster, L., Desai, S. et al. (2022). Global cross-calibration of the jason-3 and sentinel-6 michael freilich missions during their tandem period. Poster in Ocean Surface Topography Science Team Meeting 2022, Venice. doi:10.24400/527896/a03-2022.3354.

Passaro M., Cipollini P., Vignudelli S., Quartly G., Snaith H., 2014. ALES: A multi-mission subwaveform retracker for coastal and open ocean altimetry. Remote Sensing of Environment 145, 173-189, https://doi.org/10.1016/j.rse.2014.02.008.

Passaro M., Hemer M., Quartly G.D., Schwatke C., Dettmering D., Seitz F.: Global coastal attenuation of wind-waves observed with radar altimetry. Nature Communications, 12, 3812, 10.1038/s41467-021-23982-4, 2021.

Passaro M., Schlembach F., Oelsmann J., Dettmering D., Seitz F.: Coastal Assessment of Sentinel-6 Altimetry Data during the Tandem Phase with Jason-3. Remote Sensing, 15(17), 4161, 10.3390/rs15174161, 2023.

Raney, R.K., 1998. The delay/doppler radar altimeter. IEEE Trans. Geosci. Remote Sens. 36 (5), 1578–1588. https://doi.org/10.1109/36.718861.

Reale, F., Dentale, F., Carratelli, E.P., Fenoglio-Marc, L., 2018. Influence of Sea State on Sea Surface Height Oscillation from Doppler Altimeter Measurements in the North Sea. Remote Sens. 10 (7), 1100. https://doi.org/10.3390/jmse8060447.

Reale, F., Pugliese Carratelli, E., Di Leo, A., Dentale, F., 2020. Wave orbital velocity effects on radar Doppler altimeter for sea monitoring. J. Marine Sci. Eng. 8 (6), 447. https://doi.org/10.3390/jmse8060447.

Recchia, L.; Guccione, P.; Moreau, T.; Donlon, C. Exploiting the Sentinel-6 Michael Freilich Equivalent Number of Looks for Sea State Applications, submitted in Remote Sens.

Rieu, P., Moreau, T., Cadier, E., Raynal, M., Clerc, S., Donlon, C., Borde, F., Boy, F., Maraldi, C., 2021. Exploiting the Sentinel-3 tandem phase dataset and azimuth oversampling to better characterize the sensitivity of SAR altimeter sea surface height to long ocean waves. Adv. Space Res. 67 (1), 253–265. https://doi.org/10.1016/j.asr.2020.09.037.

Santos-Ferreira, A.M.; Da Silva, J.C.B.; Magalhaes, J.M. SAR Mode Altimetry Observations of Internal Solitary Waves in the Tropical Ocean Part 1: Case Studies. *Remote Sens.* 2018, *10*, 644. https://doi.org/10.3390/rs10040644.

Santos-Ferreira, A.M.; da Silva, J.C.B.; Srokosz, M. SAR-Mode Altimetry Observations of Internal Solitary Waves in the Tropical Ocean Part 2: A Method of Detection. *Remote Sens.* 2019, *11*, 1339. https://doi.org/10.3390/rs11111339.

Santos-Ferreira, A.M.; da Silva, J.C.B.; Magalhaes, J.M.; Amraoui, S.; Moreau, T.; Maraldi, C.; Boy, F.; Picot, N.; Borde, F. Effects of Surface Wave Breaking Caused by Internal Solitary Waves in SAR Altimeter: Sentinel-3 Copernicus Products and Advanced New Products. *Remote Sens.* 2022, *14*, 587. https://doi.org/10.3390/rs14030587.

M. Scagliola, L. Recchia, D. Giudici, and M. Kuschnerus, Pulse limited waveforms from interleaved mode: An analysis on the achievable speckle noise reduction, in Ocean Surface Topography Science Team Meeting 2016. Available online at: https://meetings.aviso.altimetry.fr/fileadmin/user_upload/tx_ausyclsseminar/files/IPM_05_scagliola_OSTST_2016_v3_17h15.pdf.

Scharroo, R., Bonekamp, H., Ponsard, C., Parisot, F., von Engeln, A., Tahtadjiev, M., de Vriendt, K., Montagner, F., 2016. Jason continuity of services: continuing the Jason altimeter data records as Copernicus Sentinel-6. Ocean Sci. 12, 471–479. https://doi.org/10.5194/os-12-471-2016.

Schlembach F., Passaro M., Quartly G.D., Kurekin A., Nencioli F., Dodet G., Piollé J.-F., Ardhuin F., Bidlot J., Schwatke C., Seitz F., Cipollini P., Donlon C., 2020. Round Robin Assessment of Radar Altimeter Low Resolution Mode and Delay-Doppler Retracking Algorithms for Significant Wave Height. Remote Sensing, 12(8), 1254. https://doi.org/10.3390/rs12081254.

Schlembach F., Ehlers F., Kleinherenbrink M., Passaro M., Dettmering D., Seitz F., Slobbe C.: Benefits of fully focused SAR altimetry to coastal wave height estimates: A case study in the North Sea. Remote Sensing of Environment, 289, 113517, 10.1016/j.rse.2023.113517, 2023.

Science Activity Plan, Sentinel-6 Michael Freilich and Jason-3 Tandem Flight Exploitation (S6-JTEX), Ref. CLS-ENV-NT-21-0480, Issue 1, Revision 0, 30/11/2021. https://www.s6-jtex.org/wp-content/uploads/2023/07/D-10-CLS-ENV-NT-21-0480_SAP_S6_JTEX.pdf

Taburet, N., Moreau, T., Amraoui, S., Boy, F., Characterization and exploitation of S6-MF products over in-land waters exploiting the tandem phase with Jason3, towards 3 centimetric accuracy hydrology products, submitted in Remote Sens.

Timmermans, B.; Gommenginger, C.; Dodet, G.; Bidlot, J.R. (2020a) Global Wave Height Trends and Variability from New Multimission Satellite Altimeter Products, Reanalyses, and Wave Buoys. Geophysical Research Letters, 47, 1–11. doi:10.1029/2019GL086880.

Timmermans, B.; Shaw, A.G.P.; Gommenginger, C. (2020b) Reliability of Extreme Significant Wave Height Estimation from Satellite Altimetry and In Situ Measurements in the Coastal Zone. Journal of Marine Science and Engineering. doi:10.3390/jmse8121039.

Timmermans, B., Gommenginger, C., Donlon, C., Uncertainties in sea state observations from buoys and satellite altimeters during the Jason-3/Sentinel-6 MF Tandem Experiment, submitted in Remote Sens.

P. Thibaut, L. Amarouche, O. Z. Zanife, N. Steunou, P. Vincent, and P. Raizonville. “Jason-1 altimeter ground processing look-up correction tables”, Marine Geodesy, 27(3-4): pp 409-431, July 2004. https://doi.org/10.1080/01490410490902133.

Tourain C. et al., "Benefits of the Adaptive Algorithm for Retracking Altimeter Nadir Echoes: Results From Simulations and CFOSAT/SWIM Observations," in IEEE Transactions on Geoscience and Remote Sensing, vol. 59, no. 12, pp. 9927-9940, Dec. 2021, doi: 10.1109/TGRS.2021.3064236.

Tran, N., Amarouche, L., Boy, F., 2020. Impact of the ocean waves on the Delay/Doppler altimeters: Analysis using real Sentinel-3 data. In Ocean Surface Topography Science Team Meeting 2020. Available online at https://ostst.aviso.altimetry.fr/fileadmin/user_upload/tx_ausyclsseminar/files/TranetAl_DopplerWaves_DataAnalysis_OSTST_2020.pdf.

Vayre, M., Moreau, T., Taburet, N., Borde, F., Bo, F., LeGac, S., Picot, N., Water Level Monitoring Over Continental Areas from Fully-Focused SAR Altimeter Processing, in Ocean Surface Topography Science Team Meeting 2020, Available online at: https://meetings.aviso.altimetry.fr/fileadmin/user_upload/tx_ausyclsseminar/files/OSTST2020_FFSAR_WL_01.pdf

Walsh, E.J., 1982. Pulse-to-pulse correlation in satellite radar altimeters. Radio Sci. 17, 786-800. https://doi.org/10.1029/RS017i004p00786.

Wingham, D.J., Francis, C.R., Baker, S., Bouzinac, C., Brockley, D., Cullen, R., de Chateau-Thierry, P., Laxon, S., Mallow, U., Mavrocordatos, C., Phalippou, L., Ratier, G., Rey, L., Rostan, F., Viau, P., Wallis, D., 2006. CryoSat: a mission to determine the fluctuations in Earth's land and marine ice fields. Adv. Space Res. 37 (4), 841-871. https://doi.org/10.1016/j.asr.2005.07.027.

ACRONYMS AND ABBREVIATIONS

CNES	Centre National d'Etudes Spatiales
DD	Delay-Doppler altimeter
ECV	Essential Climate Variable
ENL	Equivalent Number of Looks
ESA	European Space Agency
FFSAR	Fully Focused SAR
GCOS	Global Climate Observing System
GDR	Geophysical Data Record product
GMSL	Global Mean Sea Level
HR	High Resolution
HFMR	High Frequency Microwave Radiometer
HRMR	High Resolution Microwave Radiometer
IR	Altimeter Impulse Response
IRF	Impulse Response Function
ISW	Internal Solitary Waves
J3	Jason-3 mission
LRM	Low Resolution Mode
L1	Level 1
L2	Level 2
LIT	Lake Ice Thickness
LSE	Least-Square Estimator
MLE	Maximum Likelihood Estimator
MSL/GMSL	(Global) Mean Sea Level
MSS	Mean Sea Surface
MWR	Micro-Wave Radiometer
NR	Numerical Retracker
NTC	Non Time Critical delay
POS4	Poseidon-4 altimeter
PRF	Pulse Repetition Frequency
RMSE	Root Mean Square Error
S6-JTEX	Sentinel-6 Michael Freilich and Jason-3 Tandem Flight Exploitation
S6-MF	Sentinel-6 Michael Freilich
SAP	Science Activities Plan
SAR/SARM	Synthetic Aperture Radar (Mode)
SIC	Sea Ice Concentration
SLA	Sea Level Anomaly
SSB	Sea State Bias
SSH	Sea Surface Height
SSHA	Sea Surface Height Anomaly
SWH	Significant Wave Height
TCA	Triple Collocation Analysis
USAR	Unfocused SAR
VS	Virtual Station
WL	Water Level
WSH	Water Surface Height
WTC	Wet Tropospheric Correction

1 Introduction

1.1 Scope of the document

The "Sentinel-6 Michael Freilich and Jason-3 Tandem Flight Exploitation" study (S6-JTEX) is an ESA-funded project, to carry out a comprehensive and exhaustive analysis of the Sentinel-6MF (S6-MF) measurements during the tandem flight opportunity with Jason-3 (J3), with the aim of demonstrating the high performance achieved by this new reference mission for altimetry and monitoring of water surfaces in oceans, lakes and rivers. This study led to a wealth of scientific results, notably highlighting the benefit of the S6-MF mission in extending the legacy of sea-surface height measurements in the continuity of the Jason series. It also enabled us to exploit the full capabilities of this new reference mission, and to use innovative processing to develop new potential products and applications.

This document is the Final Report (FR) document which summarizes the main outcomes of the scientific activities that have been carried out in the framework of this project. These findings, along with the method and data used to support the different studies are described in detail in the related peer reviewed papers referenced in this document.

2 S6-JTEX Study Objectives

2.1 Objectives of the S6-MF and Jason-3 tandem flight exploitation

The Copernicus Sentinel-6 Michael Freilich (S6-MF) satellite has taken over the responsibility as the reference mission to continue the long-term record of sea-surface height measurements started in 1992 by the Topex-Poseidon satellite and then by the Jason series. The role of Copernicus Sentinel-6 Michael Freilich is not only to extend the record for climate studies, but also to monitor the changing height of the sea surface with greater precision than before, with an error on the trend of less than 1mm/year (Scharroo et al., 2016; Donlon et al., 2021).

To achieve this objective, the S6-MF satellite carries a radar altimeter of new generation, Poseidon-4 (POS4), supported by a new highly precise microwave radiometer, AMR-C (Advanced Microwave Radiometer-C). The POS4 altimeter evolves significantly from its predecessors (Poseidon-3A and -3B instruments on board Jason-2 and -3 respectively) and features higher performance than this previous generation. First it embeds a new operating mode, currently termed interleaved, that allows, for the first time, to make use of synthetic aperture radar (SAR) capability (Raney, 1998; Wingham et al., 2006; Boy et al., 2017) in the altimeter reference mission time series. POS4 also features a new architecture, increasing the use of digital functions which aims at enhancing the stability of the altimeter performances. Furthermore, POS4 performs a near continuous transmission (i.e. interleaved) of Ku-band pulses, that allows both conventional low-resolution mode (LRM) and SAR mode data to be generated simultaneously, ensuring continuity with previous pulse limited altimeter missions. This interleaved mode not only reduces the noise of SAR altimeter measurements, but also significantly improves the inter-burst coherent integration performance (an important step forward compared to the Cryosat-2 and Sentinel-3 missions which are currently impacted by sidelobes in the along-track point target response (PTR) caused by the lacunar sampling of the closed-burst operation mode as described in Egido & Smith, 2017). It is thus expected to fully benefit from the fully focused SAR (FF-SAR) processing capabilities and thus obtain much more details of the ocean surface structures, but also over sea ice areas and inland water bodies. On top of that, POS4 includes an on-board RMC processing to reduce SAR mode data volume transmitted to Earth, enabling high-resolution observations worldwide, in oceans and along the coasts, as well as over rivers and lakes for hydrology purposes.

The Poseidon-4 altimeter is designed to ensure enhanced continuity of the long time series of measurement. It is nonetheless a completely new instrument with a new architecture and new capabilities which needed to be thoroughly commissioned. Any differences or discrepancies with other missions (in particular with respect to Jason-3, along with they form a tandem flight convoy formation) had to be detected and strategies to be established to correct for any errors in the S6-MF data that might arise owing to this new radar instrument and design.

The Sentinel-6 Michael Freilich and Jason-3 Tandem Flight Exploitation (S6-JTEX) is an ESA project aimed at providing an exhaustive analysis of the Sentinel-6MF (S6-MF) measurements during the tandem flight opportunity with Jason-3 to demonstrate the high benefit of this new altimeter reference mission to extend the legacy of its predecessors. These analyses required a detailed characterization of the S6-MF POS4 instrument compared with Jason-3, a better understanding of the phenomena that can affect, corrupt, bias or noise the retrieval of the geophysical parameters of interest, and finally a better characterization of the accuracy of these measurements which is a key parameter for deriving regressions on long term series for climate applications. Different S6-MF operational modes (LRM, SAR RAW and SAR RMC) were activated during the tandem phase, but low- and high-resolution observations were performed simultaneously most of time, allowing S6-MF data to be directly cross-compared at the same surface sample location.

Another objective was to study innovative processing algorithms to enhance the exploitation of the capabilities of the mission and enable the development of new products and applications.

2.2 Objectives of the S6-MF and Jason-3 tandem flight exploitation

The science activities implemented in the S6-JTEX project are listed in Table 1. Activities organised by surfaces and processing, were carried out by a highly skill multi-partner consortium.

All results of these studies are reported to the science community in peer-reviewed journal articles, and communicated through meetings (e.g., Moreau et al., 2023), but are also available on the project website https://www.s6-jtex.org/.

Id	Title	Activity Theme	Organizations
1.1	Validation of the S6-MF measurements over open ocean and characterization of potential differences/discrepancies with respect to Jason-3	CalVal ocean	CLS
1.2	Evaluation of the performance of S6-MF measurements in coastal areas	CalVal ocean	TUM
2.2	Benefit of a second calibration phase between S6-MF and Jason-3	uncertainties and GMSL	magellium
3.1	Validation of S6-MF sea state measurements using triple collocation analysis	sea state	National Oceanography Centre
3.2	Exploiting differences and processing techniques to study ocean swell waves and high sea states and mitigate their impact on S6-MF SSH measurements	sea state	CLS
4.1	Exploiting the S6-MF effective number of looks (ENL) for sea state applications	statistical analysis of L1 data	aresys
5.1	Exploitation of Fully focused SAR (FFSAR) processing using S6-MF over ocean and sea ice surfaces	FF-SAR processing	CLS aresys
6.1	Characterization and exploitation of S6-MF and J3 in support of improved hydrology products	inland water analysis	CLS
7.1	Study of the S6-MF capability for estimating the Lake Ice Thickness	cryosphere surfaces	CLS
8.1	Study of new S6-MF capability in tandem with J3 and together with other satellite data sets to measure internal wave surface signatures over the ocean	internal waves detection study	U.PORTO

Table 1: Table of the S6-JTEX case studies.

3 S6-JTEX Scientific Studies

3.1 CalVal Ocean

On April 7th, 2022, the Copernicus Sentinel-6 Michael Freilich (S6-MF) mission took over from its predecessor, Jason-3 (J3), as the reference mission to continue recording sea-level climate data. Thanks to the 16-month duration of the S6-MF/J3 tandem flight, a large amount of spatially and temporally co-located data was collected, enabling a precise assessment of the Poseidon-4 altimeter performance with respect to J3. A complete CalVal analysis was carried out to identify any discrepancies/differences between J3 and S6-MF LR over ocean. Residuals between S6-MF LR and Jason-3 datasets were analyzed globally over ocean, but also over specific geographical areas, atmospheric conditions and sea states, in order to highlight any source of dependency. Where discrepancies were identified, they were examined in order to understand their origin and propose corrections, where necessary, to ensure a seamless transition between the two missions. Thanks to this large dataset, the level of uncertainties is low.

In March 2023, a new version of S6-MF ground segment (processing baseline F08) introduced significant enhancements for the LR mode, including the incorporation of a numerical retracker (Buchhaupt et al, 2018, Dinardo et al., 2023) alongside the historical Maximum Likelihood Estimator-4 (MLE4) retracker (Amarouche et al., 2004). In the NR, the waveform model is computed numerically using a frequency-domain formulation of the sea surface response (Buchhaupt et al, 2018), thus limiting the number of FFT (Fast Fourier Transform) operations in the iterative retracking process and making the processing computationally efficient for all timeliness with also less complexity. Cadier et al. (2024) have performed a full assessment of this new LR numerical retracker (NR) over open ocean, ranging from the outputs of these retrackers to their contribution to the Global Mean Sea Level (GMSL). Improvements relative to MLE4 are primarily observed in terms of sea-state-related effects, resulting in a 60% reduction in the bias of the S6-MF/J3 Sea Surface Height Anomaly (SSHA) correlated to Significant Wave Height (SWH) as shown in Figure 1. This outcome enhances the already strong continuity between the two missions.

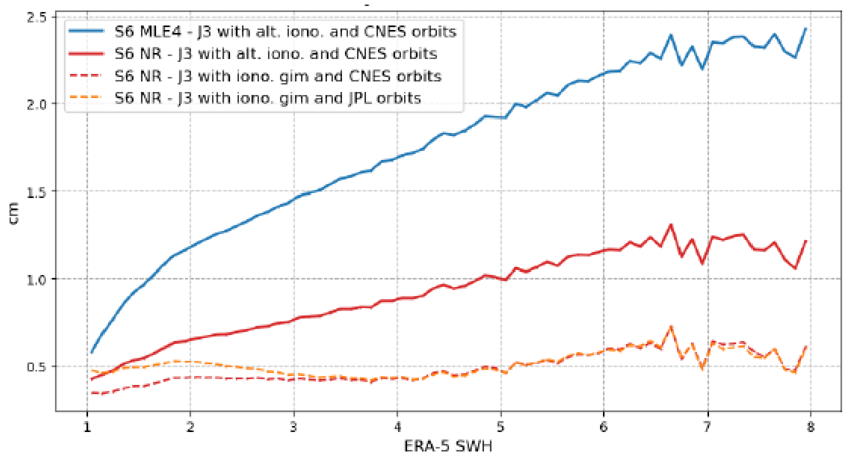

Figure 1: SSHA difference: S6-MF LR minus J3 MLE4 as function of ERA5 SWH. Computed over POS-4B tandem flight for ERA5 SWH greater than 1 m (Cadier et al., 2024)

The assessment of S6-MF NR reveals an excellent overall performance, with high data availability and outlier proportions comparable to those of other altimetry missions. With an SSH error at crossover of only 3.3 cm, it demonstrates precise measurements. S6-MF retracker errors align closely with MLE4 and NR, exhibiting values below J3 by 2 mm on the range and by 2 cm on SWH. Direct comparisons of S6-MF parameters with J3 during the tandem phase reveal good continuity, albeit with minor discrepancies attributed to various system components such as orbit, radiometer wet troposphere correction, C-band processing, or an MLE4-based empirical adjustment. Unlike MLE4 retracker, S6-MF NR retrievals do not require correction via the instrumental LUT (Thibaut et al., 2004), which eliminates potential calculation errors. The S6-MF NR allows to greatly reduce the correlation with SWH to just 3 mm. This is a major improvement for the continuity between J3 and S6-MF as reference missions in the climate record of sea level. The remaining correlation may be, at least in part, linked to the pulse-to-pulse correlation effect affecting the S6-MF LR data.

Cadier et al. (2024) also pointed out that the application of a new C-band SSB table dedicated to S6-MF could further mitigate discrepancies. This may not remove the residual bias between the S6-MF and J3 ionospheric corrections, but it will at least provide an SSB correction consistent with the S6-MF C-band. In addition, it has been shown that the stability of SSHA bias is influenced by platform restarts and radiometer WTC instability, impacting the long-term stability of GMSL analysis. Finally, a 60-day signal, linked to the beta-prime angle, is observed on both the SSHA bias tracking and the GMSL difference (Figure 2). This behavior is linked to the S6-MF CNES POE-F orbit (product orbit), as described in Nilsson et al. (2022). The improvement of the S6-MF NR in terms of long-term stability cannot be assessed in this study due to the short time series available at the time of writing, but also due to the stability of the POS-4B altimeter.

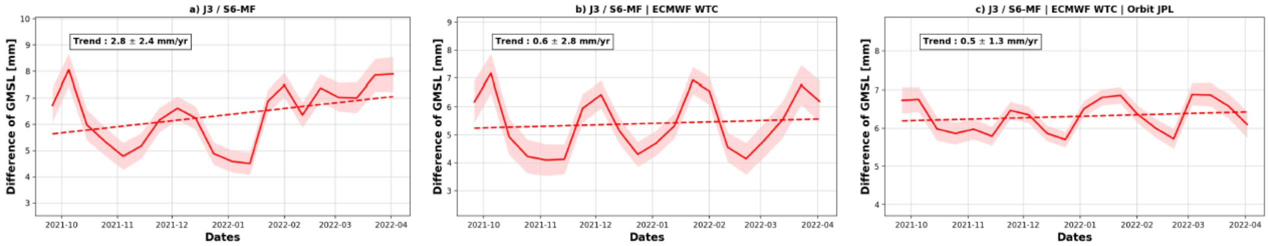

Figure 2: GMSL differences between J3 and S6-MF LR NR over the side B tandem phase using the radiometer and CNES orbits (a), model and CNES orbits (b), model and JPL orbits (c) (Cadier et al., 2024)

The transition from POS-4A to POS-4B introduces discontinuities, warranting the reassessment of Ku-band external path delay and the use of NR retrievals for precise adjustments. In-depth analyses are needed to address discrepancies and ensure seamless continuity in sea level climate records between the two missions. The use of a NR for the C-band could also bring benefits to this regard.

Another notable feature of the S6-MF NR is its use of the in-flight Point Target Response (PTR) in the waveform modeling to mitigate instrumental drift (induced by potential instrument's ageing), thereby enhancing long-term stability. The GMSL analysis presented in Cadier et al. (2024) indicates no significant trend difference compared to J3, once the impact of the radiometer wet troposphere correction is accounted for.

3.2 Coastal study

The accuracy of altimetry measurements in the coastal areas is affected by the local departure of the radar signal from the known ocean response (due to inhomogeneities of the illuminated area) and the inaccuracy of the corrections, as well as of the tidal models, needed to isolate anomalies in the sea level variability (Cipollini et al., 2017).

Sea Surface Height (SSH) from Delay-Doppler (DD) instruments is generally more precise and reliable in the coastal zone if compared to previous standard low-resolution mode (LRM) altimetry missions, even without any specific coastal retracker. Despite the improvements, the quantity and the quality of sea state and sea level retrievals in the coastal zone is still significantly different than from the open ocean. For example, concerning Significant Wave Height (SWH), it has been observed that the amount of missing data and outliers in Sentinel-3 data for a distance to coast of less than 20 km amounts to almost 40% (Schlembach et al., 2020).

In the latest years, the reprocessing of Low-Resolution Mode (LRM) missions using specific coastal retracking algorithms such as ALES retracker (Passaro et al., 2014) has shown that meaningful information can be retrieved in general up to 3 km from the coast and in some cases until few hundreds of meters (Benveniste et al., 2020). Such retracker improves the detection of sea level in the coastal zone by overcoming the difficulties in retrieving the information from contaminated radar waveforms. Despite the improvements made, these methods are not yet part of the ground segment of LRM missions and reprocessings, with the consequence that DD coastal performances are compared with LRM data that are not optimized for the coastal zone.

Given that the coastal zone is explicitly an objective of S6-MF, there is a need to understand how reliable the data provided to the users are and what are the improvements compared to the coastal-optimized LRM data. Moreover, in view of future reprocessings, the best strategy concerning possible additional dedicated retrackers and the different modes of operations have to be found. In this respect, Passaro et al. (2023) assessed the coastal capabilities of J3 and S6-MF altimeters during their tandem phase, comparing the operational products from different processing modes (LRM, SAR-RAW and SAR-RMC) as well as data reprocessed using waveform retracking methods tailored for coastal applications. Their performances have been evaluated considering the quality of retrievals (outlier analysis), their precision (along-track noise analysis), potential systematic biases, and accuracy (comparison against tide gauges). It is to be notes that all the statistics are referred to the 20-km limit from the global coastline, i.e. the area in which typically the general performance of satellite altimetry data is considered degraded.

Two main conclusions emerge from this study. Firstly, the official SAR altimetry products of S6-MF provide superior coastal monitoring capabilities than those based on LR mode (from J3 and S6-MF). In particular, it has been shown that the official S6-MF SLA product derived from SAR altimetry offers an 8% improvement in correlation analysis (see Figure 3). Secondly, Passaro et al. (2023) showed that dedicated coastal retracking can notably enhance SAR altimetry performance. Regarding specific processing methods, we observed that the ALES retracker for S6-MF LR (ALES LR) exhibits lower precision than its J3 counterpart, indicating the need for further investigation into implementation issues and mission differences. Additionally, the J3 Adaptive LR retracker (Tourain et al., 2021), known for improving mesoscale signal-to-noise ratio globally, enhances SWH data precision but performs less accurately against ground truth for sea level determination near the coast.

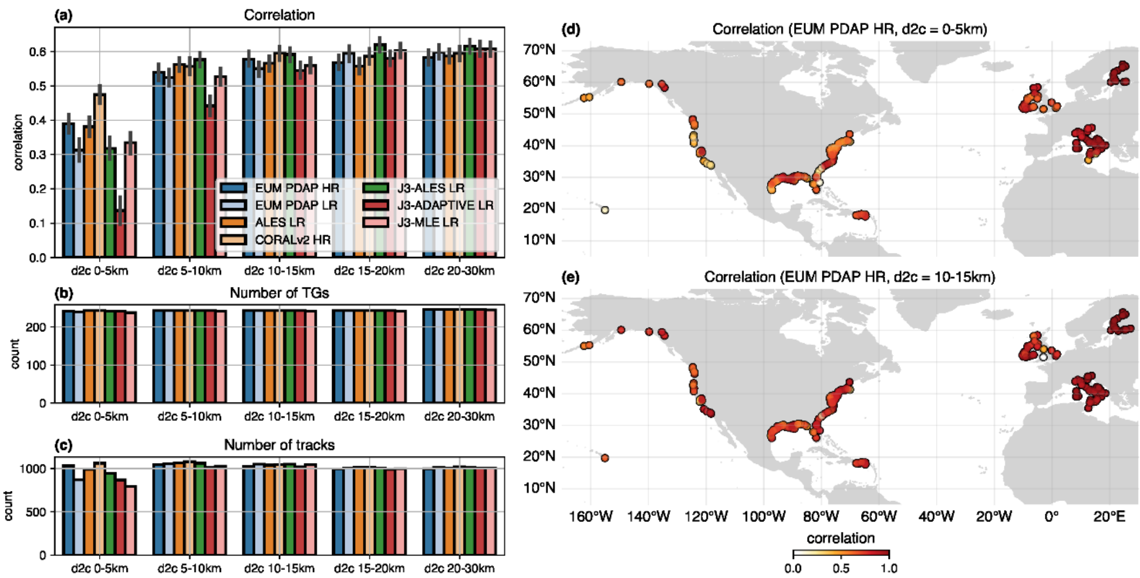

Figure 3: (a) Mean correlations (with 90% confidence intervals) per dataset and distance to coast; (b,c) Number of tide gauges and total number of available tracks for which correlations are computed. These numbers are also an indication of how many data are available in the different datasets; (d,e) show the best correlation per tide gauge for different distances to the coast and for the PDP HR dataset. One station located west of Hawaii is not shown in (d,e), (Passaro et al., 2023).

In summary, our main conclusion is that the official PDP HR SAR altimetry product achieves coastal performance comparable to that of an improved coastal altimetry reprocessing of LR data (ALES LR, J3 ALES LR), with potential for further improvement using a dedicated subwaveform approach applied to the same SAMOSA physical model (CORALv2 HR). These findings highlight the significance of dedicated coastal retracking algorithms for enhancing the capabilities of both traditional, pulse-limited altimeters and more recent developments utilizing SAR altimetry.

3.3 Study for improved uncertainties in GMSL estimates

Tandem flight phases have played a key role in verifying and ensuring the consistency of sea level measurements between successive altimetry reference missions (TOPEX/Poseidon (TP), Jason-1, Jason-2, Jason-3, and more recently Sentinel-6 Michael Freilich (S6-MF). It enables us to measure the relative errors between the two altimeter missions. By averaging random errors over several months, we can assess the systematic instrumental errors and perform an accurate calibration of both altimeter missions. On the global scale, the uncertainty in the global mean sea level offset is approximately +/- 0.5 mm ([16-84]%). However, the detection of instrumental drift is difficult during a tandem phase due to its short duration (9 months to 1 year).

The study described in Ablain et al. (to be submitted) aims to propose a novel validation method with a better ability to assess the long-term stability of altimeter parameters in sea level estimates. The proposed validation method is based on the implementation of a second tandem flight phase between two successive satellites. The principle of the method consists first of reevaluating the systematic instrumental errors during the second tandem phase a few years after the initial tandem phase. The trend between the systematic errors made during the two tandem phases is then calculated to assess the stability of the altimeter parameters over the entire period that covers both tandem phases. In this study, we develop a robust method to estimate the uncertainty of the trend to analyse the ability of the second tandem phase to detect a drift. We calculate the uncertainty of the two tandem phase validation methods on the global scale, depending on the duration of the second tandem phase and on the time elapsed between the two tandem phases. We also calculate the uncertainty of the two tandem phase validation methods at regional scales, analysing the sensitivity to the spatial scales from a few hundred to a thousand kilometres. Finally, we compare the results obtained with other validation methods to highlight the benefits of the second tandem phase for assessing the long-term stability of the altimeter parameters.

The results are discussed considering the first tandem phase between Jason-3 and Sentinel-6 Michael Freilich missions (September 2021 - March 2022) and with regard to the scenario foreseen for the second phase between Jason-3 and S6-MF planned for early 2025, 2 years, and 9 months after the end of the first tandem phase. On the global scale, we demonstrate that the second tandem phase validation method allows us to assess the stability of the altimeter parameters with an uncertainty of approximately +/- 0.15 mm yr^{-1} ([16-84]% confidence level) as shown in Figure 4. The uncertainty increases to +/- 0.4-0.6 mm yr^{-1} at regional scales of 2000-4000 km ([16-84]% confidence level).We also show that a reduction in uncertainties is significantly more sensitive to the time elapsed between the two tandem phases than to the duration of the second tandem phase, and we recommend a minimum duration of 4 months for the second tandem phase. Conducting regular double tandem phases between successive altimetry missions would be a valuable approach to accurately evaluating the altimeter parameter stability in the future.

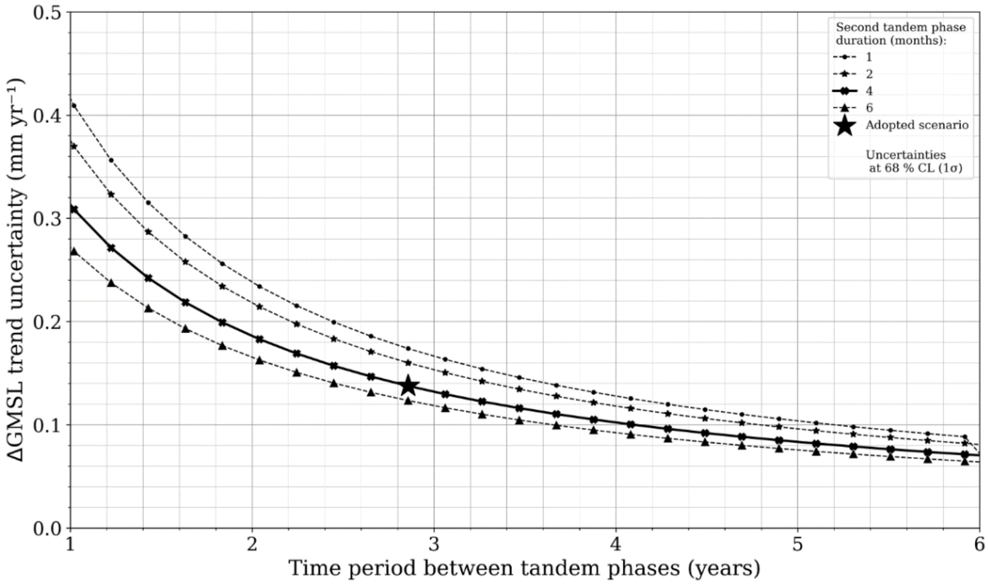

Figure 4: Evolution of the uncertainty of the trend in GMSL differences (ΔGMSL) with the time elapsed between the two tandem phases between Jason-3 and S6-MF for several durations of the second tandem phase, ranging from 1 month to 6 months. The scenario adopted by the spatial agencies for the second tandem phase, which is four months long and separated by two years and nine months from the first, is indicated with a star (Ablain et al., to be submitted).

3.4 Validation of S6-MF sea state measurements

The Sentinel-6MF/Jason-3 Tandem provided a unique opportunity for in-depth investigations of the uncertainties and error characteristics of altimeter sea state data. Given the high temporal and spatial variability of sea state, standard inter-comparison methods (e.g. cross-overs) are unable to isolate the contributions to observed uncertainties due to natural variability, random instrument errors and systematic instrument/processing biases. In the case of S6-MF, with its key role in ensuring long-term continuity of the altimeter reference data record, understanding these uncertainties and the consistency of its sea state measurements in the context of other satellites, and in different ocean conditions, is particularly critical (Timmermans et al. 2020a,b). The S6-MF/Jason-3 Tandem gave the opportunity to evaluate, for the first time, the performance of the new S6-MF SAR Interleaved mode (Gommenginger et al., 2013) directly against S6-MF LRM and J3 (LRM), and to explore the relative merits of difference modes and satellites (biases, random errors, continuity) in different oceanic conditions (e.g. high waves, swell, low winds).

In this study, Timmermans et al. (2024) scrutinized the consistency and uncertainties associated with the sea-state altimeter measurements collected in both modes, in the northeast Pacific region, using standard statistical methods and a triple collocation analysis that both include independent in situ fiducial data and global models as in (Clerc et al., 2020). Comparisons revealed minimal differences in mean significant wave height (Hs, 0.01 m) and root-mean-square deviation (0.06 m) between J3 and S6-MF LR, although disparities with buoy data were notable. While S6-MF HR data shows a high correlation with LR data (0.999) (see Figure 5), it does exhibit a nonlinear sea state-dependent bias. The bias can be explained effectively through regression modeling based on Hs.

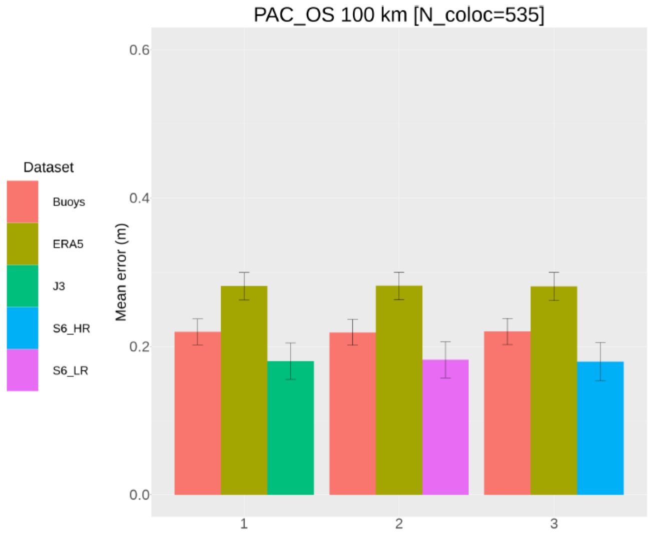

Figure 5: Error variances from TCA for each of the tandem datasets compared with buoy data and ERA5 reanalysis. Uncertainty in the result is denoted by black bars showing 1 s.d. (Timmermans et al., 2024).

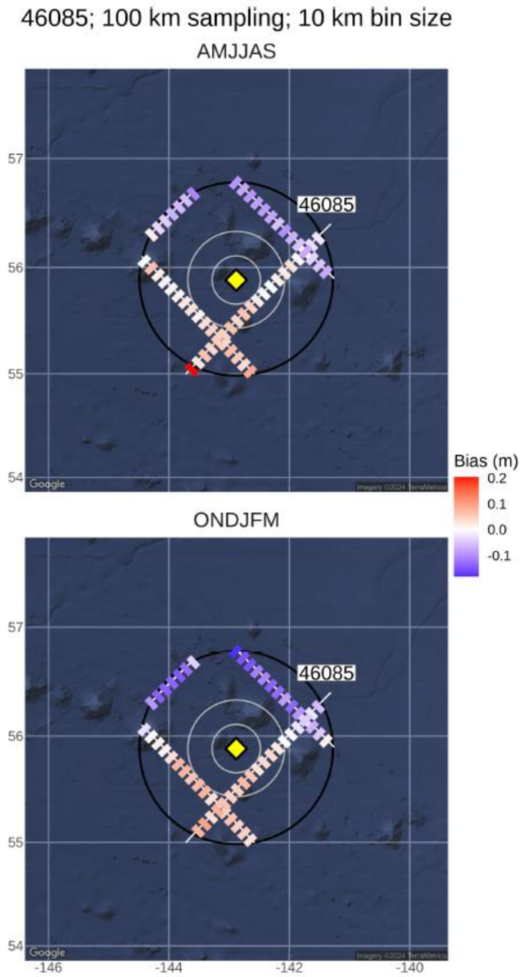

Figure 6: Seasonal Hs mean bias (AMJJAS, top panel; ONDJFM, bottom panel) between J3 and buoy 46085 is shown for the period 2017 to 2021. A spatial gradient is readily apparent, being strongest in the winter months. Notice that, in ONDJFM in particular, the points along the altimeter tracks closest to the buoy show a positive bias, rather than zero (Timmermans et al., 2024)

Subsequent triple collocation analysis (TCA) indicated negligible differences in error variances (~0.18+/-0.03 m) for the three altimetry datasets, buoy data, and ERA5 reanalysis. However, the limited statistical precision due to the total collocations (N=535) both complicates interpretation and motivates the use of a larger dataset. This study also identified uncertainties in the collocation methodology, with important consequences for methods such as TCA. In particular, data from some commonly used buoys are found to be statistically questionable, possibly linked to erroneous buoy operation. Additionally, we developed a methodology (based on the work of Timmermans et al., 2020b) that shows how statistically anomalous altimeter data may arise due to local sea state gradients (effect seen in **Erreur ! Source du renvoi introuvable.**). These results, described in Timmermans et al. (2024) have important consequences for validation of observations and the study of sea state variability. They further highlight the interest of this method to improve the collocation accuracy closer to the coast, by providing a larger number of possible collocation samples and greater statistical robustness. A full implementation, currently ongoing, will offer new insights into the use of HR altimetry for such analyses.

3.5 Sea State study: ocean waves dynamics

Since the launch of CryoSat-2, the first altimetry mission with a delay/Doppler mode, and its operating over some ocean areas, various researchers have been interested in understanding the delay/Doppler measurements sensitivity to ocean surface characteristics including waves geometry and dynamics. This research intensified with the arrival of Sentinel-3 A&B and Sentinel-6 and their operating of delay/Doppler mode over the globe. Several conclusions have been drawn so far. The estimated ocean surface parameters are sensitive to the period and energy of long ocean waves. but also, on their orientation with respect to the satellite track (Aouf et Phalippou, 2015; Abdalla and Dinardo, 2016; Moreau et al., 2018; Reale et al., 2018; Rieu et al., 2021). Another important effect of swell is the increase of the high-frequency noise on the estimated parameters, but also of the Sea Surface Height variance at longer wavelengths because of the aliasing (Reale et al., 2020; Rieu et al., 2021). In addition, to this swell effect, orbital velocities (Boisot et al., 2016; Buchhaupt, 2019; Egido et al., 2019b, Amarouche et al., 2019; Tran et al., 2020) induced by all the sea states and not limited to swell only, can also alter the delay/Doppler signal leading to estimation biases in SWH data which can in turn induce a bias in SSH estimates through the SSB correction. Other phenomena can furthermore affect the delay/Doppler measurement leading possibly to additional biases in SSH estimation. They may be related to nonlinear effects of waves leading to upwave/downwaves sensitivity of SSH and SWH estimates (Tran et al. 2020). More recently, a sensitivity of the range to wind speed direction was observed using Sentinel-3 data and then confirmed with Sentinel-6 data (Cadier et al., 2022). Tran (2021) analyzed this sensitivity and found a clear correlation of this range bias with wind waves propagation direction with respect to the satellite track. Due to Sentinel-6 altimeter characteristics (higher illumination time than Sentinel-3 and CryoSat-2), sea state effects on the estimates have been found higher.

The aim of the present work (Amarouche et al., to be submitted) was to further assess the potential impact of ocean wave conditions and dynamics on the long-term sea state and sea level time-series of Sentinel-6 MF and to propose approaches to mitigate negative SSH impacts due to delay/Doppler processing and reduce regional biases that would enter into the sea level record. This analysis focused on the impact of the vertical velocities, the wind speed and direction, Stokes drifts and total surface currents.

To this end, we used one year of real Sentinel-6MF data and information on waves and currents from the ERA5 and MERCATOR models. A theoretical analysis was also carried out to explain the observed behavior. The results of the real data analysis combined with the theoretical analysis enabled us to conclude that delay/Doppler measurements are influenced by the combination of three phenomena: waves orbital velocity, wind speed (inducing roughness asymmetry between upwaves and downwaves) and along-track Stokes drifts.

More specifically, we found that HR estimates of range are affected by sea state, wind speed (total amplitude and not only the along-track component), orbital velocity and Stokes drifts in the satellite along-track direction. In particular, we demonstrated that the observed correlations of HR and LR range differences with wind direction are in fact due to the correlation between wind and Stokes drifts (see Figure 7). We also found that the total surface currents in the along-track direction have a very limited impact on the HR range compared to Stokes drifts impact (see Figure 7 on the right).

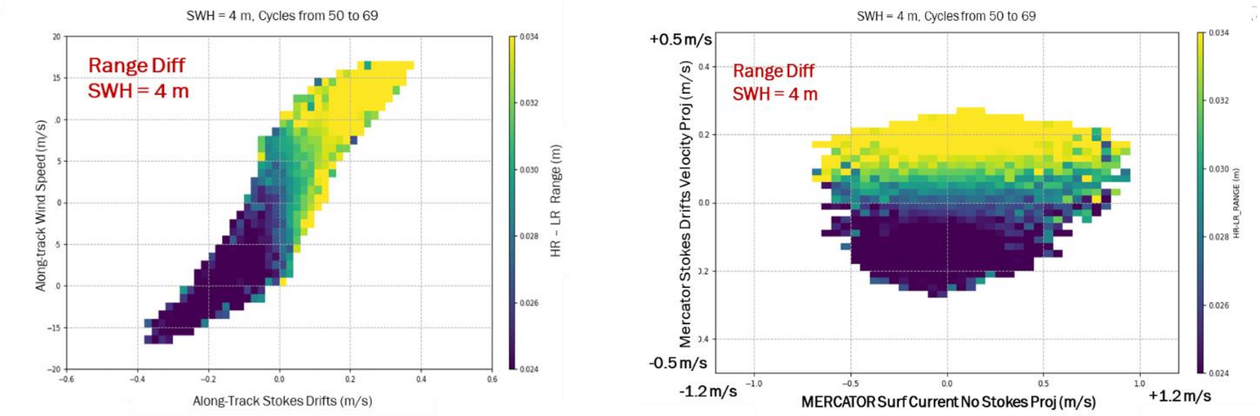

Figure 7 Range difference between HR and LR modes for SWH = 4 m wrt. along-track Stokes drits and along-track wind speed (left) and wrt. along-track surface total currents excluding Stokes drits and along-track Stokes drifts (right), (Amarouche et al., to be submitted).

For what concerns SWH, we found that HR estimates of SWH are affected by an error linked to sea state, waves orbital velocity and the total amplitude of wind speed (Figure 8).

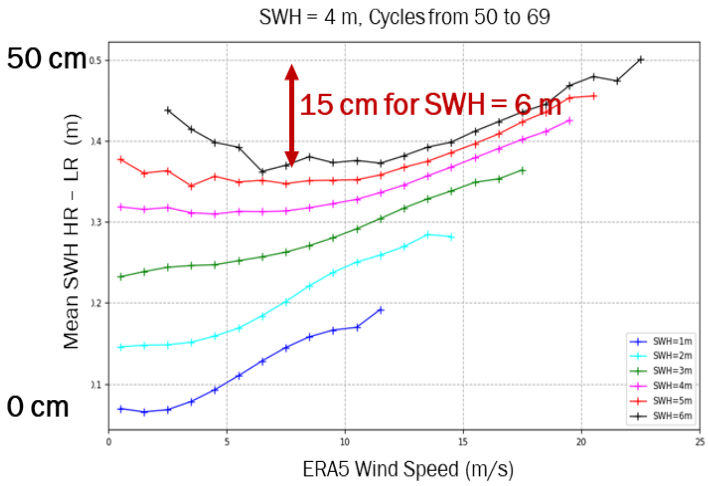

Figure 8 SWH difference between HR and LR modes for SWH ranging from 1 to 6 m wrt. along-track Stokes drits and along-track wind speed (left) and wrt. along-track surface total currents excluding Stokes drits and along-track Stokes drifts (right), (Amarouche et al., to be submitted).

Recommendations have been made for the development of two new corrections, one for SWH and the second one for the range or SSH. The SWH correction using SWH, orbital velocity and wind speed should provide improved results over the Egido et al. (2022) correction thanks to the addition of wind speed. The correction of the range can be considered as a generalized sea-state bias or pseudo sea-state bias correction, as it includes the classic SSB correction but also the other surface effects that affect the Doppler signal: SWH, wind speed and mean wave period as already done in the current SSB 3D model developed for conventional altimetry but adding along-track Stoke drifts (and orbital velocity with lower priority). This latter requires the development of a new SSB correction mathematical method. This work is on-going at CLS, independently from this study. As soon the new regression method is available, we recommend developing a new SSB or pseudo SSB correction for delay/Doppler measurements.

3.6 Statistical analysis of level-1 data

This study aimed at verifying the existence of a discrepancy in S6-MF geophysical parameters obtained starting from low-resolution mode waveforms because of the higher pulse repetition frequency. While conventional low-resolution mode altimeters like J3 operates at PRF around 2 kHz, S6-MF operates at PRF around 9 kHz, so that, according to the results in (Egido and Smith, 2019a; Clerc et al., 2020), significant sea-state-dependent biases are expected introduced during the retracking. Initial studies on the correlation properties of consecutive pulses from nadir-looking pulse-limited radar altimeters were primarily focused on determining the maximum pulse repetition frequency at which statistical independence could be achieved (Walsh, 1982). Following these studies, the pulse repetition frequency (PRF) for the Jason series was selected to be approximately 2 kHz.

Copernicus Sentinel-6 Michael Freilich is the first altimeter operating in a continuous high-rate pulse mode, i.e. interleaved mode. This design enables the simultaneous production of low-resolution mode measurements with a pulse repetition frequency of ~9KHz for the Ku-band. S6-MF thus leads to an elevated number of highly correlated individual echoes compared with the lower number of Jason-3 altimeter echoes that are only slightly correlated. Recent studies (Scagliola, 2016; Egido and Smith, 2019a) have revealed that for LRM waveforms, averaging a larger number of correlated individual echoes (~18KHz) yields a higher Equivalent Number of Looks (ENL) compared to averaging a fewer number, weakly correlated echoes (~1.8KHz). Furthermore, it has been shown that despite the fact that the noise in the estimation of geophysical parameters is reduced at higher PRFs, the dependence of statistical properties on the range gate introduces significant biases in the retracked parameters using a least-square estimation approach. These biases depend on the sea state and must be properly taken into account to ensure continuity of sea level monitoring between S6-MF and Jason-3, the new and previous reference missions in the ocean surface topography satellite series.

In this study, Recchia et al. (2024) first theoretically evaluated the correlation properties of the S6-MF pulse limited waveform echoes, then validated the model by comparing it to the ENL empirically estimated using real data for different ocean conditions. The ENL has also been calculated for different decimation cases with respect to the original S6-MF PRF, confirming the higher number of looks gained with a 9kHz acquisition system, even when partially correlated waveforms are taken (see Figure 9).

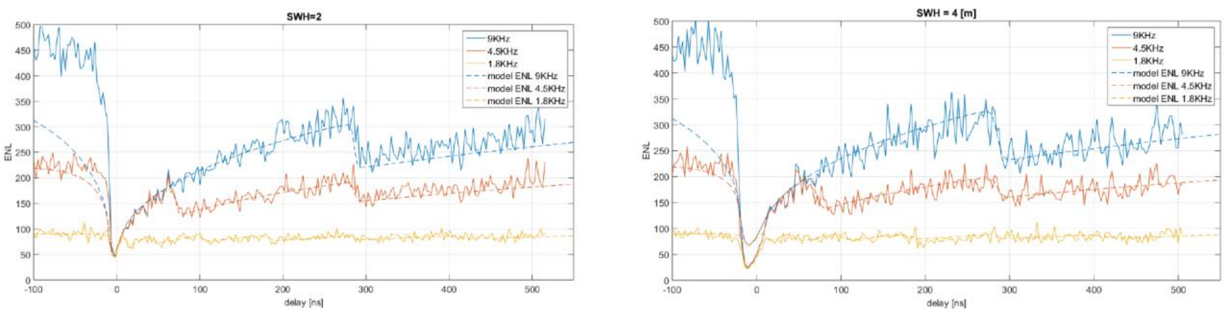

Figure 9: ENL values for SWH = 2m (left panel) and SWH = 4m (right panel), using open ocean S6-MF data. ENL (solid-line) is plotted as a function of the delay time (in samples) and different decimation factors; the corresponding theoretical trend is in dashed line ENL (Recchia et al., 2024).

This work has enabled us to verify the existence of a significant range dependence of the statistical properties for the S6-MF low-resolution mode waveforms, and to assess its impact on the precision and accuracy of geophysical parameter estimation, confirming results reported in Dinardo et al., 2023. It is important to point out here that increasing the PRF improves the precision of the measurements but introduces estimations biases if non-optimal estimation methods are used. These biases could be corrected empirically using a look-up-table or more elegantly and appropriately, using a Maximum Likelihood Estimators (MLE). This is crucial for the S6-MF mission, which aims to provide, as a reference mission, highly accurate time series of sea level measurements.

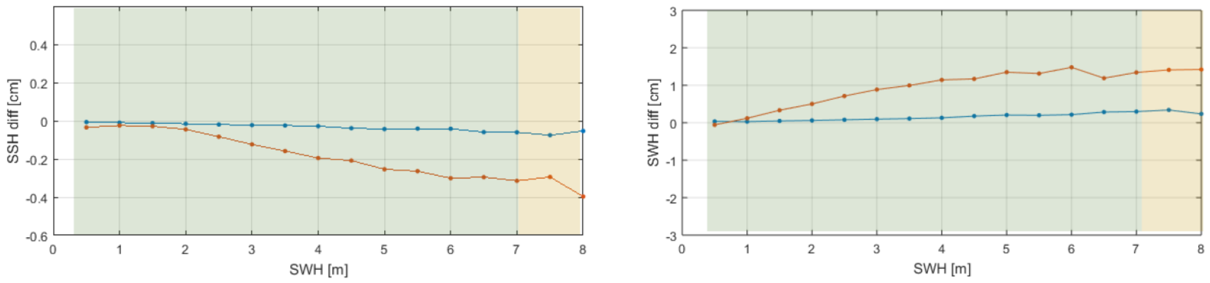

Figure 10: Bias of S6-MF SSH (left panel) and SWH (right panel) for two different decimation factor w.r.t. the original PRF, as a function of the SWH. Blue lines: bias between 9kHz and 4.5kHz (factor 2); red lines: bias between 9kHz and 1.8kHz (factor 5). The shaded green area is where more than 2000 observations were available; in the orange area less than 2000 were available (Recchia et al., 2024).

3.7 Fully-Focused SAR processing study

Fully-focusing of radar altimeters is a recent concept that has been introduced in Egido and Smith (2017) to allow further improvement of along-track resolution in high pulse repetition frequency (PRF) radar altimeters. While in Delay/Doppler processing the coherent summation of pulses is performed over a limited number of successive pulses (i.e., bursts), the concept of coherent summation has recently been extended to the whole synthetic aperture. This is the so-called fully-focused synthetic aperture radar (FFSAR) concept, in which all the echoes within the antenna extent are coherently summed after phase compensation to increase the along-track resolution up to its theoretical limit (half the along-track antenna length) and to improve also the ENL with respect to Delay/Doppler.

The exploitation of FFSAR waveforms in scientific applications is still in its infancy (Kleinherenbrink et al, Egido et al, 2020; 2020; Vayre et al., 2020; Altiparmaki et al., 2022). In addition, the high PRF radar altimeters already in operation (CryoSat-2 and Sentinel-3A/B) have design features (emitting pulses in closed burst) that do not allow optimal exploitation of the FFSAR processing, preventing the development of FFSAR-based applications to date. Indeed, the closed burst acquisition mode implies the presence of grating lobes in the along-track FFSAR Impulse Response Function (IRF), which reduce the achievable accuracy of the resulting geophysical parameters. In addition, the deramping-on-receive instruments introduce along-track phase distortion that needs to be properly characterized and then compensated for in order to obtain sufficient quality in the FFSAR waveforms.

S6-MF Poseidon-4 instrument offers new capabilities to investigate on the real potential of FFSAR concept. Thanks to the open-burst acquisition mode of the Poseidon-4 instrument, grating lobes are no longer present (at least at levels well below those observed on closed-burst altimeters). Additionally, the matching-filter-on-receive scheme of Poseidon-4 guarantees greater phase coherence within the visibility time of each point target. On the other hand, the use of a lower PRF (9kHz) in Poseidon-4 compared to previous altimeters at 18kHz induces Doppler ambiguities that affect the FFSAR waveforms in the case where the entire Doppler bandwidth is processed.

Amraoui et al. (2024) demonstrate the outstanding ability of the S6-MF FFSAR to observe small-scale patterns with unprecedented resolution in altimetry. In particular, it has been shown that this processing, when properly configured (Doppler bandwidth, integration time and along-track windowing), significantly enhances the observation of specular and diffuse targets, thereby opening up a multitude of possibilities for monitoring various types of surfaces, including open ocean, hydrology, and sea-ice, all of which are expected to benefit immediately from it. This work also led to the determination of a set of configuration parameters, along with recommendations for replica mitigation and posting rates, to enable optimal processing of S6-MF FFSAR data for these different surfaces.

Among the most significant findings, it has been demonstrated that windowing is crucial for enhancing the signal-to-noise ratio on specular targets, despite potentially compromising resolution. It is noteworthy that surfaces with anisotropic scattering characteristics act as natural windowing, affecting resolution. Additionally, replicas (induced by the two missing Ku pulses in the pulse transmission scheme) pose a challenge on specular surfaces, and various techniques like deconvolution or peak signature identification have been proposed, albeit with implementation complexities and inconsistent results. The method developed in Amraoui et al. (2024), based on complex single-look summation, effectively eliminates replicas but also removes incoherent targets, arising from destructive interference as shown in Figure 11. The applicability and benefits of this method have yet to be assessed on a larger data set.

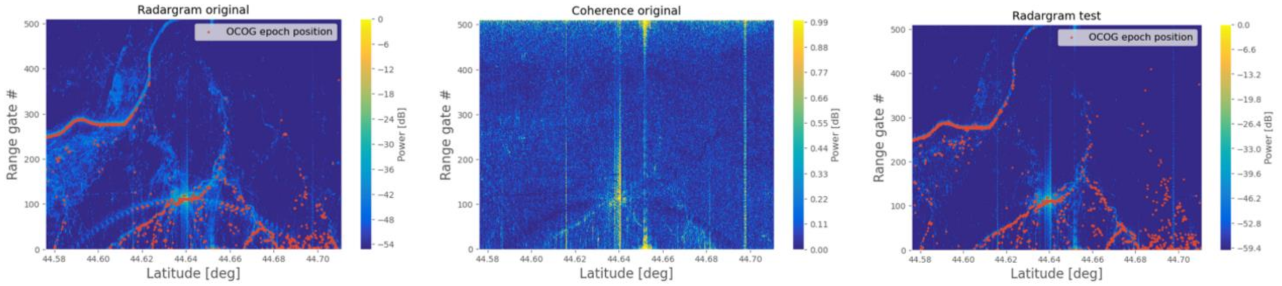

Figure 11: Illustration of the replicas removal strategy on S6-MF over the Garonna river. The left panel is the original radargram at 500 Hz, the middle panel is the corresponding coherence and the right panel is the radargram multiplied by the coherence (equivalent to the sum of the complex single-looks). Red dots represent the epoch gate position from the OCOG retracker (Amraoui et al., 2024).

On non-specular targets, addressing the aliasing issue specific to the S6-MF mission involves reducing the Doppler bandwidth and integration time proportionally. Also, multilooking is essential, especially in open-ocean areas, to reduce speckle noise and identify wave modulation crucial for generating 2D spectra in FFSAR radargrams. For satisfactory noise reduction (80%), we recommend a posting rate between 150 Hz to 200 Hz or equivalent ground sampling between 46 m and 34 m.

The high-resolution along-track data from FFSAR allows visualization of altimeter radargrams as folded images, enabling application of pattern recognition techniques developed for SAR imagery techniques to possibly extract valuable new information from the surface that is not accessible from conventional LR and SAR data, complementing waveform retracking outputs, and thus expanding altimetry applications (as in Hernández-Burgos et al., 2024). One of those findings concerns the ability of FFSAR data to image long-wave modulations at the sea surface, and the confirmation that the left/right ambiguities are due to folding of the backscattered signal in nadir-looking altimetry, as demonstrated for the Madeira case study (see Figure 12). In this example, as the S6-MF track passes along the coast of the island, the altimeter sees only one side of the flight track (very weak signals are backscattered by the island), enabling the unambiguous determination of the wave field direction (except for the uncertainty in the forward/backward direction inherent in imagery) as shown in Figure 13.

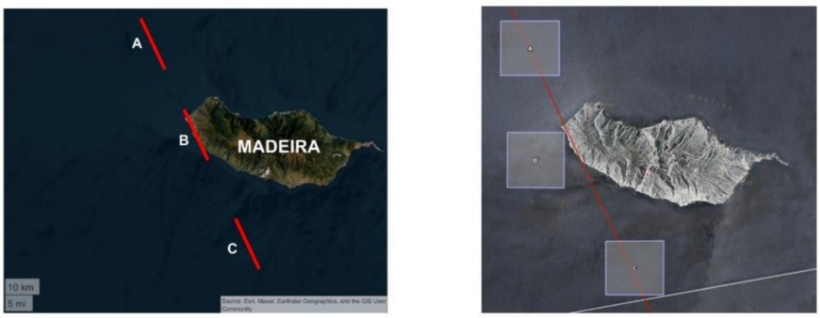

(**a**) Sentinel-6 Michael Freilich track (**b**) Sentinel-1A image

Figure 12: The Madeira island scene overflown by S6-MF and S1A. The S6-MF track is shown in red, overlaid on (a) an image of the island and (b) the S1A image. The analysis is divided into three zones: after, over, and before the island (A, B, and C respectively). The corresponding coverage is shown by the red lines in (a) for S6-MF and by the boxes for (b) for S1A. (Amraoui et al., 2024).

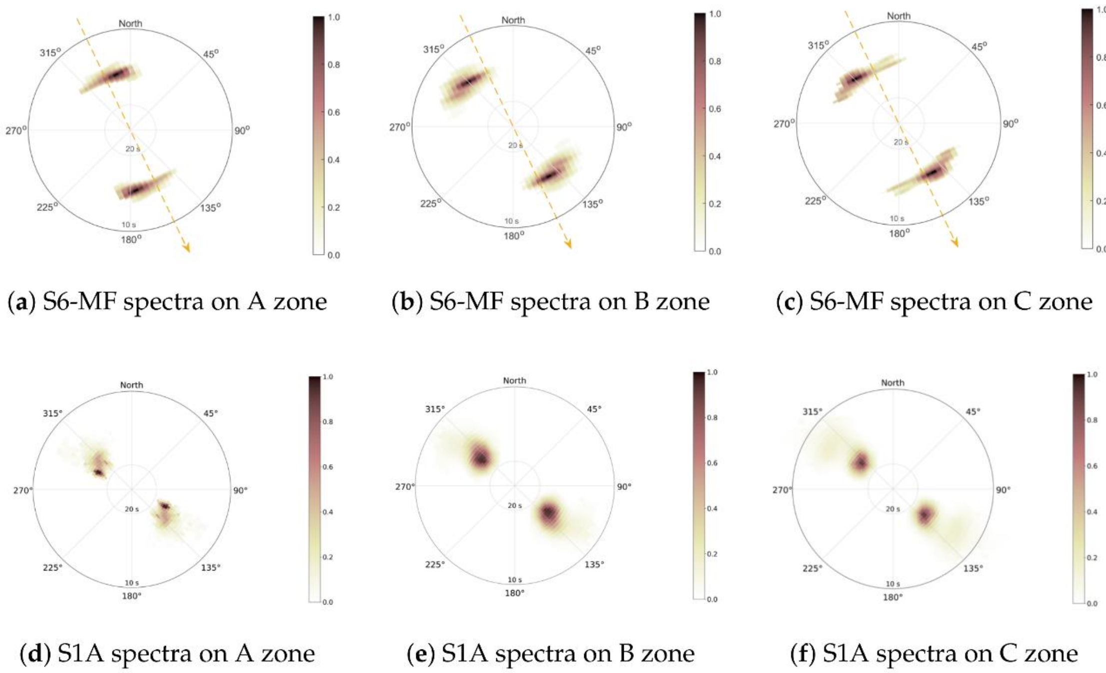

(**a**) S6-MF spectra on A zone (**b**) S6-MF spectra on B zone (**c**) S6-MF spectra on C zone

(**d**) S1A spectra on A zone (**e**) S1A spectra on B zone (**f**) S1A spectra on C zone

Figure 13: Two-dimensional modulation spectra computed for S6-MF (first row) and S1A (second row). The first, second and third columns correspond, respectively, to A, B and C zones (Figure 12). The S1A spectra are plotted in polar grid while S6-MF spectra are in cartesian grid (Amraoui et al., 2024).

Furthermore, the exploration of the potential of the S6-MF FFSAR radargrams in detecting sea-ice leads, primarily through single-look coherence, revealed the ability to identify thin leads (<100 m), which is of great interest for observing polar sea surfaces during ice transition. FFSAR processing demonstrates even thinner lead identification compared to S1, suggesting applying S1 lead detection algorithm directly to FFSAR radargrams.

3.8 Inland Water analyses

Validating Sentinel-6 MF measurements over inland waters and characterizing any discrepancies or differences compared to Jason-3 are crucial to ensure seamless continuity for operational monitoring services (e.g., Copernicus Global Land Lakes and Rivers Water Level Service) as well as for climate applications (e.g. Copernicus Climate Change Service, Copernicus Climate Initiative Lakes). In this regard, Taburet et al. (2024) performed a comprehensive comparison of water level retrievals over inland waters in between S6-MF and J3, with a particular focus on the SAR data of the S6-MF mission.

First, direct comparisons in between the altimetry dataset were performed to quantify the bias in between S6-MF SAR WSH retrieval with OCOG with J3 WSH retrievals (with ice1). It was performed over lakes to address a large range of sigma0 values – linked to surface size and roughness – and we showed the SAR-LRM bias strongly depends on the transect size (see Table 1). The S6-MF SAR WSH (OCOG) – J3 WSH (ice1) median bias ranges from -24cm over short transects (<600m) to + 9cm over the largest lakes. We point out that the -24cm bias over specular targets should be accounted for by users when building Jason-S6-MF timeseries.

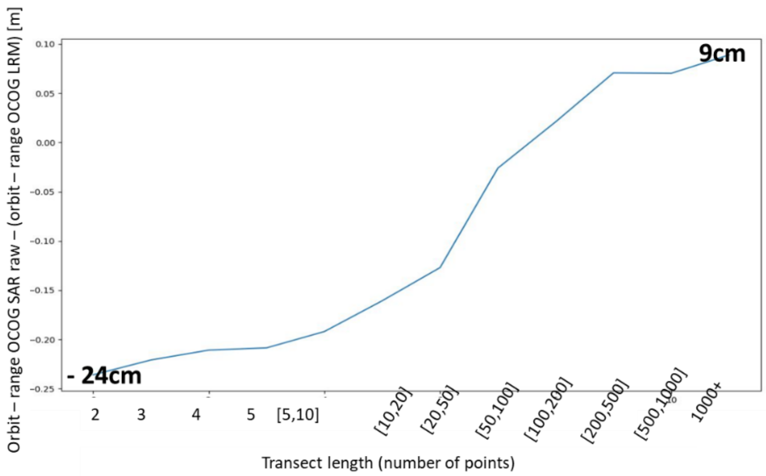

Figure 14: Median of (orbit-range) differences in between SAR RAW and LRM per transect size classes. 2 stands for transects containing 2 points, hence of length 300 to 600m (Taburet et al., 2024).

Then, comparisons of J3 and S6-MF reconstructed water level timeseries to insitu water level timeseries over French rivers were performed. We stressed the benefit of the 6 months long tandem phase in RMC mode to provide enough points of comparisons of the two missions with insitu timeseries to compute robust statistics. The improved precision of SAR mode compared to LRM was emphasized: over ideal cases (flat rivers without surrounding contaminating water bodies) water level estimation improves from 17cm with J3 to 2.3cm with S6-MF SAR RMC. When considering more complex scenes as the one presented in Figure 15, where factors such as river slope cannot be perfectly accounted for, performance improvement is still significant from 29 cm u-RMSE with J3 down to 9.7 cm with S6-MF SAR over a set of 12 virtual stations presenting a favourable geometrical configuration covering rivers from 10 m to 300 m width.

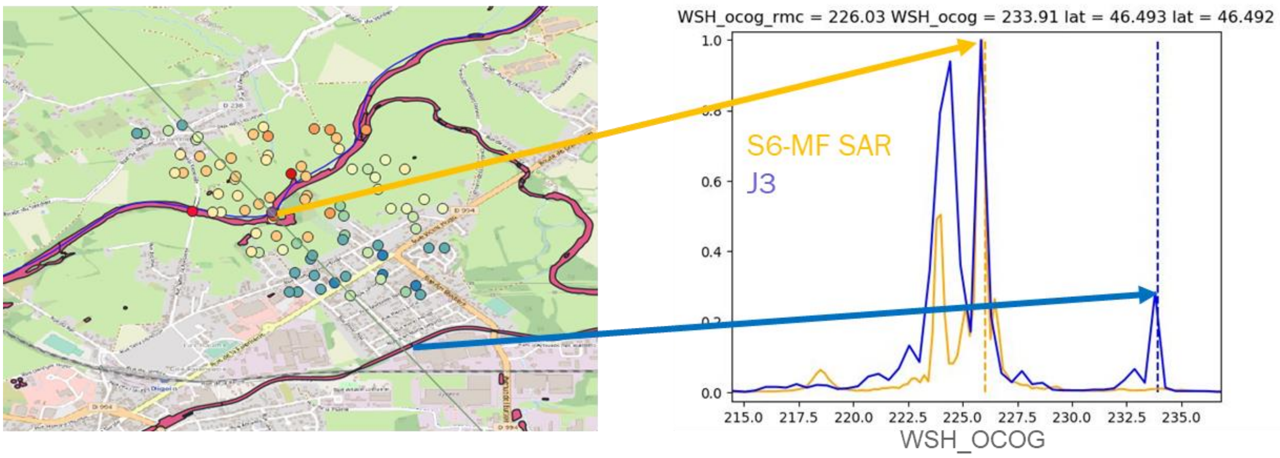

Figure 15: Comparisons of S6-MF SAR (in yellow) and J3 (in blue) waveforms at the nadir of the Arnoux river at Digouin (about 40m wide). The points of the map represent the Sentinel-6 L2 data selected at the nadir of the river, they span a large area due to satellite excursion in between cycles around its reference track. The yellow/green color gradient indicates the S6-MF sigma0 estimates from the OCOG retracker. The in-situ station position is represented with the red dot. The green line is the theoretical ground track, to which the SAR band is orthogonal. The magenta dot represents the position of the virtual station at the intersection of the river centerline and the theoretical ground track (Taburet, internal communication in project)

Nevertheless, the most complex river cases show that when slope information is unknown, which prevents from correcting from the satellite 1 km deadband excursion around the theoretical ground track, and/or contamination from surrounding water bodies arises, the performances of S6-MF with respect to

J3 cannot be exploited to improve precision with respect to insitu ground truth. This leads us introducing an important novelty that consists in introducing a new type of virtual stations exploiting not only altimetry data over the rivers but also measurements acquired off-nadir water bodies. This is specific to exploiting SAR altimetry data as the SAR band geometry allows precisely targeting some sections of the rivers. We showed this processing improves precision in WSH timeseries and reduces the number of outliers with SAR mode, which is even reinforced with the application of SAR specific processing technics better focusing the signal along track such as Hamming filtering or even Fully Focus SAR.

3.9 Lake Ice Thickness analyses

The Lake Ice Thickness (LIT) is an important climate indicator, recognized as an Essential Climate Variable (ECV) by the Global Climate Observing System (GCOS). Yet, a robust and continuous monitoring of this variable is not currently available as field measurements are sparse in both geographical coverage and time. Because of the wide availability of data in terms of spatial and temporal coverage, radar altimetry has a great potential to provide with long LIT timeseries needed for climate monitoring, making it the preferred dataset for LIT climatology. However, this potential has not been fully explored so far. Significant improvements in the LIT estimation were recently shown in (Mangilli et al 2022) when using a physical based analytical retracker for the analysis of Ku-band Low Resolution Mode waveform data. While this work paved the way towards fulfilling the ambitious GCOS requirements for LIT, further improvements can still be achieved by using data at higher spatial resolution, that is, the Synthetic Aperture Radar (SAR) data.

Within this project, we developed a novel and efficient analytically based retracking approach for estimating LIT from high-resolution Ku-band (13.6 GHz) SAR altimetry data. The retracker method is based on the analytical modeling of the SAR radar echoes over ice-covered lakes that show a characteristic double-peak feature attributed to the reflection of the Ku-band radar waves at the snow-ice and ice-water interfaces (as illustrated in Figure 16). The method is applied to Sentinel-6 Unfocused SAR (UFSAR) and Fully Focused SAR (FFSAR) data, with their corresponding tailored waveform model, referred to as the SAR_LIT and FF_LIT retracker, respectively. We carried out the LIT analysis with Sentinel-6 UFSAR data at 20 Hz, and with UFSAR and FFSAR data at 140 Hz. We validated the SAR_LIT and FF_LIT retracker analysis with thermodynamical LIT simulations and with LIT estimates obtained from Sentinel-6 and Jason-3 conventional altimetry data at 20 Hz for two ice seasons during the tandem phase of the two satellites. Assessing the consistency between SAR based and LRM based LIT retrievals is important to ensure the continuity of the measurements issued from past, current and future radar altimetry missions, for robust LIT climatology and monitoring. Consistency checks of the Sentinel-6 SAR LIT estimates are also performed using optical/radar images that provide information on the snow/ice conditions on the same dates.

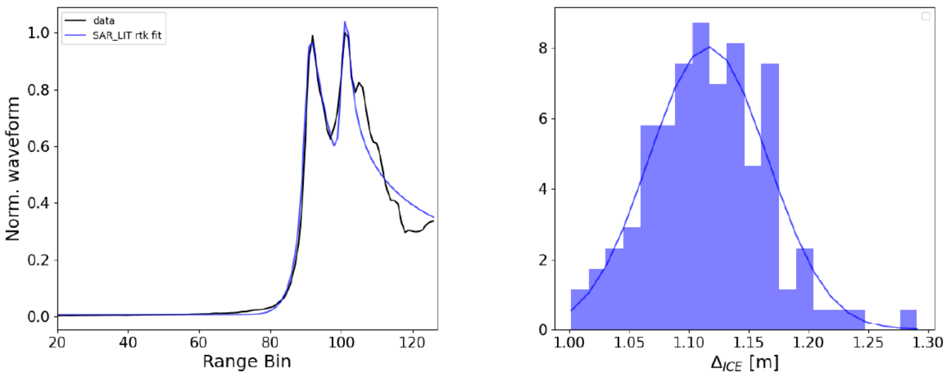

Figure 16: Example of S6 UFSAR waveform with, in blue, the SAR_LIT fit (left) and LIT histogram, with the corresponding Gaussian fit (right), in the RoI over the Great Slave lake in February 2021 (Mangilli et al., 2024).

The analysis has been performed over Great Slave Lake and Baker Lake (Canada), which differ in terms of lake size, bathymetry, snow/ice properties, and seasonal evolution of LIT. The results (as shown in Figure 17) demonstrate the capabilities of the SAR_LIT and FF_LIT retrackers to retrieve robust LIT measurements for different seasons and different type of lakes. These estimates are fully compatible with the ones obtained with LRM data, confirming the continuity of the LIT measurements and timeseries from conventional altimetry missions and current and future SAR altimetry missions. The typical LIT uncertainty obtained with the SAR_LIT retracker is in the order of 5 cm, when the ice is well established over the lake, representing a significant improvement with respect to previous studies. As expected, the LIT is estimated with significantly higher accuracy, a factor of 2 to 3 better, when using Sentinel-6 UFSAR data at 20 Hz with respect to LRM data, because of the increased resolution. The FFSAR processing at 140 Hz allows to have even more precise LIT measurements, with ~20% smaller uncertainties. The LIT retracker analysis performed on data at higher posting rate (140 Hz) shows an increased performance with respect to the 20 Hz data, especially at the melting transition, because of the increased statistics (a factor of seven more data points and therefore a higher spatial sampling of the surface).

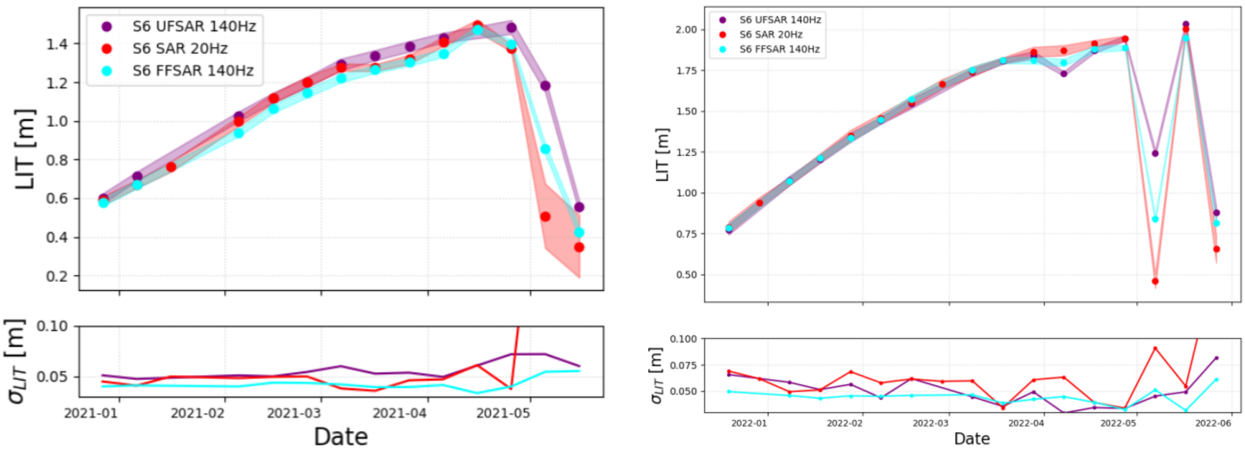

Figure 17: Example of the comparison of the LIT estimations obtained with Sentinel-6MF high resolution SAR data for one ice season over the Great Slave lake (left) and the Baker lake (right). The curves refer to Unfocused SAR at 20 Hz (red), Unfocused SAR at 140 Hz (purple) and Fully Focused SAR at 140 Hz (cyan) (Mangilli et al., 2024).

As already pointed out by (Mangilli et al 2022), the main limitation of LIT retrackers based on Ku-band waveform data is that the retracker works if the ice related signature is present. Indeed, the freshwater ice signature depends on the properties and thickness of the snow pack and the ice layer and could be erased if some conditions are not met, as for instance in the case of melting snow on the ice surface or snow-free lake ice. For this reason, the the SAR_LIT and FF_LIT retrackers can capture the seasonal transitions of ice melting but cannot precisely follow the ice evolution at the transitions because of the difficulty of retracking heterogeneous surfaces when the snow on the ice surface begins to melt. Also, there could be lakes for which the ice signature is not clearly marked or not present (as for example snow-free lakes) and therefore consistent LIT estimations and timeseries cannot be generated for these targets. Overall, when the LIT signature is present in the radar waveforms, the SAR_LIT and FF_LIT retrackers can precisely capture the seasonal LIT evolution and the inter-annual LIT variability, making them powerful tools for robust LIT estimations for climatology and monitoring.

The method and the results obtained within the project are reported in (Mangilli et al. 2024).

3.10 Internal Waves detection study

Internal waves are characterized by large-amplitude vertical displacements (typically 50-150 meters) near the largest density gradient in the water column. Their energy propagates for hundreds of kilometers perpendicularly to their crests, from generation sites near steep underwater topography to eventually breaking nearshore or dissipating offshore. They are also characterized by significant vertical velocities, mixing and associated vertical fluxes. These have implications in biological productivity and biomass observable from satellites, and can crucially affect the ocean up to the climate scale.

Recent work (Magalhaes and da Silva, 2017; Santos-Ferreria et al, 2018; 2019: 2022; Magalhaes et al., 2021) demonstrates that internal waves can be observed by satellite altimetry. Subsurface internal waves alter the ocean surface roughness that is imprinted in sigma0 signatures as well as SWH impacts at small-scale (1-3 kms) to medium-scale (10s of kms). This study focused on an analysis of the signature of internal waves in SAR and conventional altimetry data by inter-comparing S6-MF and J3 in tandem together with other satellite data sets (e.g. Sentinel-3 OLCI/SLSTR, Sentinel-2 MSI and Sentinel-1 SAR images) following similar approach as in Magalhaes et al. (2021). Different case studies were examined where seas are known hotspots for ISWs, such as in Banda Sea (see Figure 18).

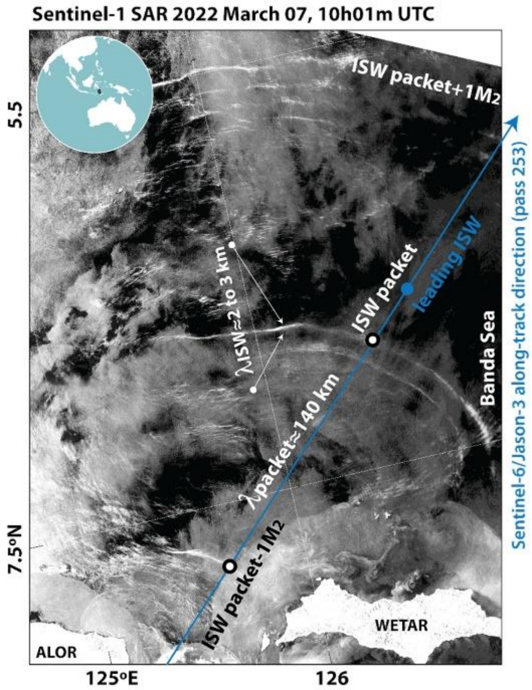

Figure 18: Sentinel-1 image over the Banda Sea (see inset in top-left corner) acquired 7 March (2022) at 10h01m UTC. Three ISW packets are seen propagating to the north/northwest separated by typical semidiurnal periods and wavelengths (i.e., from −1M2 to +1M2, with packets separated approximately by $\lambda_{packet} \approx$ 140 km). Note that, the width of the leading ISWs in each packet (λ_{ISW}) is around 2 to 3 km. For reference, the ground-track of S6-MF/J3 is shown in a blue line for pass 253 and the blue circle marks the location of the leading ISW-like signals highlighted in Figure 19 (Magalhaes et al., 2023).

Magalhaes et al. (2023) have shown that radar backscatter between S6-MF and J3 is consistently either negatively or positively correlated in Internal Solitary Waves (ISW) -like signals, when using the standard MLE4 (Amarouche et al., 2004) or the alternative ALES (Passaro et al., 2014) / Adaptive (Tourain et al., 2021) retrackers in J3 (respectively). This result is essentially a consequence of the intrinsically different acquisition geometries between SAR and conventional altimeters, since sharper along-track resolutions in S6-MF (of about 300 m) can sample the details of ISWs structure, whereas larger footprints in the conventional J3 (typically a few kilometres wide) cannot.

Although apparently of limited scope, this result may have a wider significance in satellite altimetry, since the ocean surface is far less uniform in the finer scales that SAR altimetry is now pursuing when compared with the traditional larger scales of conventional altimetry. ISWs demonstrate that in this study as they break the assumption of a uniform Brown surface in their sharp transitions between smooth and rough sections. However, other ocean phenomena can yield similar results—namely, fronts, variable surface wind, and other small-scale phenomena that can potentially affect the kilometre-scale (or less) altimetry measurements. It can then be wondered how past, present, and future altimeters —with potentially different acquisition geometries—can be reconciled towards the spatially shorter and temporal higher frequencies of the ocean spectrum. To this end, a lesson learned is that alternative algorithms such as the ALES and the Adaptive retrackers, which explore more focused views of the conventional waveforms (namely in the leading edge), can perform in the same level of SAR altimeters when dealing with sharp transitions in ocean radar backscatter (at least down to the kilometre scale) as shown in the level-2 products (for σ0, SSHAs and SWHs) presented in Figure 19. Whichever the case, the tandem phase between Sentinel-6MF and Jason-3 (likely to be one of a kind) seems to hold the key to reconciling an upcoming era of SAR altimeters with a climatological record of conventional altimetry. On a different note, it became clear that a recommendation from this study is that Jason-class level-2 products provide SSHAs also at 20 Hz (similarly e.g., to σ0 or SWH).

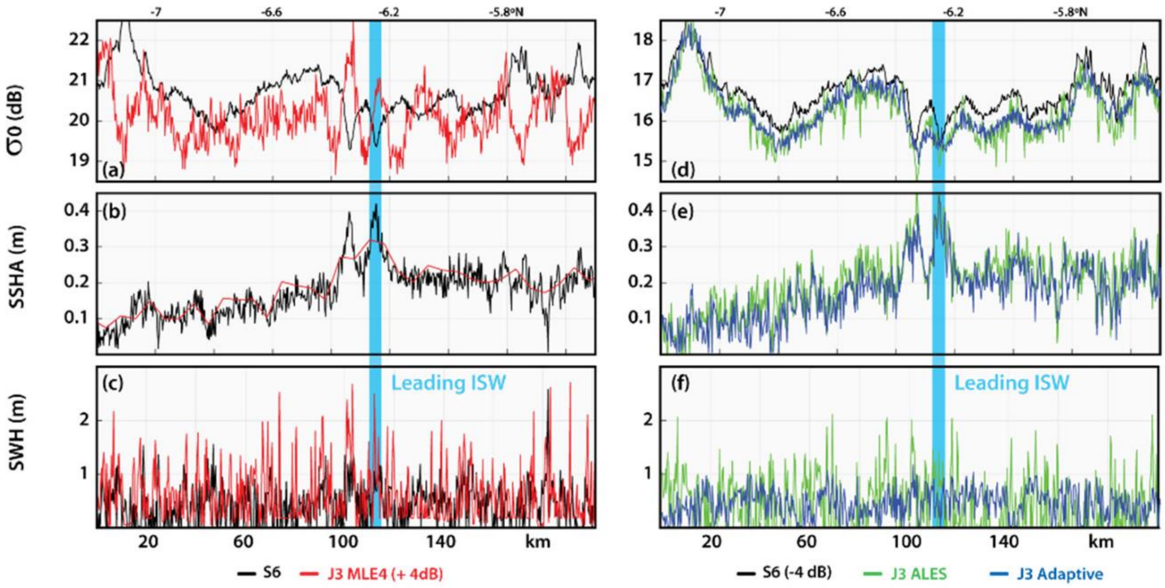

Figure 19: Panels (a-c) show σ0, SSHAs and SWHs obtained from Sentinel-6MF (S6) and Jason-3 (J3) MLE4 level-2 products (at 20 Hz, except SSHAs for MLE4) in the Banda Sea (8 March 2022). The radar backscatter from Jason-3 (J3) is shown with an offset to highlight its opposite modulations in the vicinities of the ISWs (leading ISW marked with a blue rectangle). Panels (d-f), same as previous panels for Jason-3 processed with ALES and the Adaptive retrackers (at 20 Hz). Note that panel (d) also shows the radar backscatter from Sentinel-6MF with an offset to highlight its correlation with the ALES and the Adaptive retrackers (Magalhaes et al., 2023).